ESR Study of γ-Ray Irradiated Potassium Hexacyanocobaltate $K_3[Co(CN)_6]$

Naoki FURUTA,* Tokuko WATANABE, and Shizuo FUJIWARA

Department of Chemistry, Faculty of Science, The University of Tokyo, Hongo, Bunkyo-ku, Tokyo 113

(Received October 2, 1975)

ESR results for γ-irradiated $K_3[Co(CN)_6]$ in powder and single crystal forms are reported. The main paramagnetic species detected at 77 K were diisocyanide $[Co^{II}(CN)_4(NC)_2]^{4-}$ and pentacyanocobaltate(II) $[Co^{II}(CN)_5]^{3-}$. On annealing, diisocyanide was lost and pentacyanocobaltate was formed. In Part I the reaction mechanism is discussed from the results of the powdered sample and in Part II the noncollinear structure is presented as the plausible molecular form of diisocyanide from the results of the single crystal.

The central diamagnetic transition metal ions in inorganic complex compounds are transformed into paramagnetic ones by high energy radiation, leaving the mother lattice almost unchanged. The products have been referred to as the hot ions.[1] Hot ions of Zn and Cd in cyanocomplexes have recently been investigated extensively as single crystals.[2-5] The cyanocomplexes are useful as the samples of the investigation of hot ions because they easily form good single crystals and show interesting features, such as the dimer formation and the high ligand lability; thus, cyanocobaltate(III) has been taken as the sample of the present experiment. The cyanocabaltate(II) complexes are dimerized when synthesized by the usual chemical methods, forming a diamagnetic compound. Also, the hot ion Co(II) presents ESR data which refer to the low spin state of d^7, in contrast to the usual method. It has been reported that the paramagnetic diisocyanide $[Co^{II}(CN)_4(NC)_2]^{4-}$, (to be referred to as species I),** and the pentacyanocobaltate $[Co^{II}(CN)_5]^{3-}$ (species II) are produced by the high energy irradiation of cyanocobaltate.[6-9] However, those investigations in the literature are preliminary and leave several problems to be investigated. For example, when the sample is annealed from 77 K to room temperature, only species II can be observed, and not I. Also, the mechanisms of the formation and the temperature dependence of the stability of these species have not been clarified. Hence, we decided to investigate these problems more in detail; we found that species I and species II are stable at 77 K, but, on annealing, an electron is released from species I resulting in the formation of species II. The first part of this paper is concerned with the investigation of the powdered sample, and the second part, that of the single crystal.

Part I Powdered Sample

Experimental

Potassium hexacyanocobaltate(III) was prepared with cobalt(II) chloride hexahydrate and potassium cyanide.[10] The reagents used were of the reagent grade and no further putification was done. The purity of the synthesized sample was checked by elemental analyses: Calcd for $K_3[Co(CN)_6]$: C, 21.68; H, 0; N, 25.29%. Found: C, 21.65; H, 0; N, 25.74 % mol wt 332.25. The powdered samples were exposed to γ-rays from a ^{60}Co source of the University of Tokyo at room temperature and at 77 K. ESR spectra were obtained with a JEOL 3BS Type X-band spectrometer using 100 kHz field modulation. The magnetic field was calibrated by Mn^{2+} (doped in MgO) and the resonance position of DPPH (g= 2.0036). The ESR spectrum was measured for each specimen before irradiation and it was confirmed that the sample did not contain any ESR-active paramagnetic species. The number of the hot ions was determined by comparing the integrated intensity of hot ions with that of the standard sample $[Co^{III}(NH_3)_6][Cu^{II}Cl_5]$ which contained 1.3×10^{18} Cu(II) ions. The sample was sealed *in vacuo* (4.2×10^{-6} Torr), and this was compared to the sample in air in order to see the atmospheric effect. The sample irradiated at 77 K was annealed gradually, and ESR was measured during this procedure. The effect of the total dose applied to the sample was also examined. When the sample was kept at constant temperature, species I decayed and II was formed. The rate of this decay and that of the formation were also measured.

Results

Figure 1 shows the ESR spectra of the sample after irradiation at 77 K (referred to as I in the figure) and that at room temperature (II). In both spectra $g_{//}$ and $g_{\perp}$ are split into eight lines by Co(II) with a nuclear spin of 7/2. The spectral patterns are different, with the different parameters shown in Table 1. Apparently,

Table 1. ESR parameters of hot ions formed in γ-irradiated powder $K_3[Co(CN)_6]$.

	$g_{//}$	$A_{//}$(G)	$g_{\perp}$	$A_{\perp}$(G)
Irradiated at 77 K (Spectrum I)				
$[Co^{II}(CN)_4(NC)_2]^{4-}$	2.001 (±0.002)	61.7 (±0.3)	2.091 (±0.001)	−70.0 (±0.3)
$[Co^{II}(CN)_5]^{3-}$	2.004 (±0.005)	89 (±2)	2.170 (±0.003)	−29.3 (±1)
Irradiated at room temperature (Spectrum II)				
$[Co^{II}(CN)_5]^{3-}$	2.004 (±0.005)	89 (±2)	2.170 (±0.003)	−29.3 (±1)

the features of the spectrum in Fig. 1 are complicated and cannot be analysed by simple observation. After the analysis of the angular dependence of the ESR spectra of the single crystal, it was revealed that the tensors of g and A for species I were orthogonal to each other, and $g_{//}$ was split by $A_{\perp}$ and $g_{\perp}$ by $A_{//}$ and $A_{\perp}$. More details of the latter finding will be described in Part II of this article. For species II the $A_{//}$ can be observed as

* Present address: Department of Chemistry and Physics, National Institute for Environmental Studies, P. O. Yatabe, Tsukuba, Ibaraki 300-21.

** With respect to the real form of the molecule, it is not clear whether two of the cyanide ligands are inversed[14] or twisted.[8,9] We use the formula $[Co^{II}(CN)_4(NC)_2]^{4-}$ for convenience.

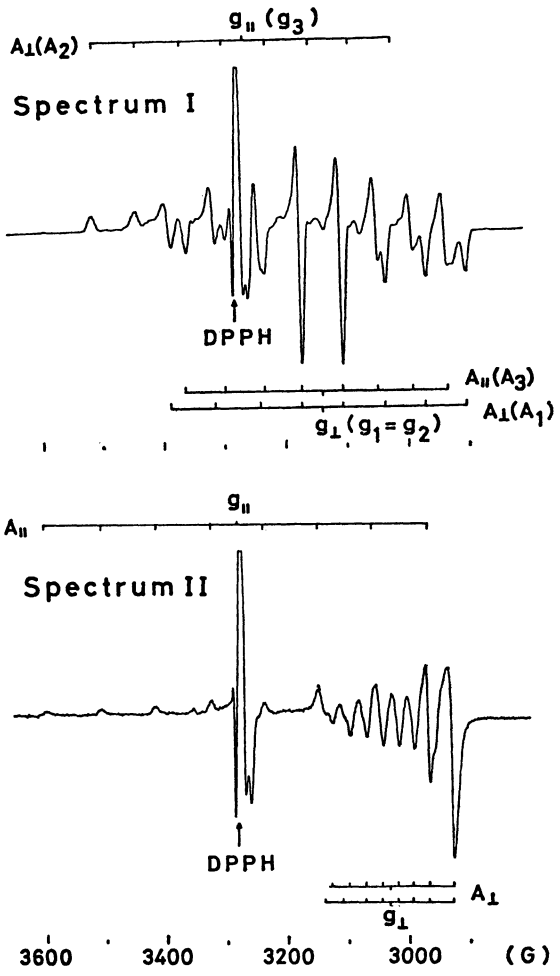

Fig. 1. ESR spectra of γ-irradiated powder $K_3[Co(CN)_6]$ at 77 K (Spectrum I) and room temperature. (Spectrum II).

the split of the $g_{//}$ part, as usual. Species I can be assigned to the hexacoordinated species $[Co^{II}(CN)_4(NC)_2]^{4-}$ and species II to the pentacoordinated one $[Co^{II}(CN)_5]^{3-}$, by the comparison of the g and A values with those of the alkylisocyanide complexes.[11,12] The temperature dependence of the two species was noticeable. As the sample which has been irradiated at 77 K was annealed to room temperature, the formation of the species II was observed by ESR. During annealing both species I and II were observed simultaneously: I decreased and II increased. The results are shown in Fig. 2. Species I decreases and II increases with time. Besides species I and II, an ESR signal of narrow linewidth was observed in the center of the spectrum; this was attributed to the radical produced by irradiation. Since the intensity of the radical species was independent of the decay of I, hence, it was not taken into the consideration of the reaction mechanisms of I and II. No sizable difference was observed between the samples sealed *in vacuo* and that in the air.

The magnitudes of the total dose exerts a large influence on the yield of hot ions, as seen in Table 2. The experimental results can be summarized as: i) on irradiation of the same dosage, the total yield of I and II is independent of the temperature, and ii) on annealing, some part of species I changes into the diamagnetic species. Figures 3 and 4 present the process of the decay and formation of hot ions. The formations of species II and the diamagnetic species are second order reactions, and the activation energies of the two reactions were measured as 9 and 8 kcal/mol, respectively.

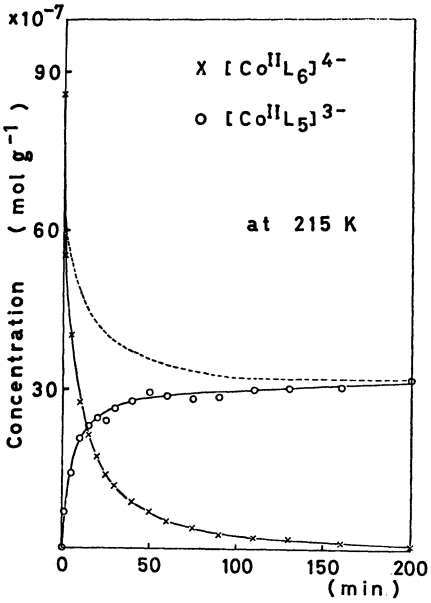

Fig. 2. The process of the decay and the formation of hot ions at 215 K.
(×: Species I, ○: species II, ----: total paramagnetic species.)

Table 2. Dose effect (×10⁻⁷ mol g⁻¹)
I: $[Co^{II}(CN)_4(NC)_2]^{4-}$
II: $[Co^{II}(CN)_5]^{3-}$
III: diamagnetic species

Total dose (rad)	Irradiated at 77 K				At r.t.
	I	II	After annealing		II
			II	III	
1×10^5	4.8	0.2	3.8	(1.2)	5.8
5×10^5	18	0.8	13	(5.8)	18
1×10^6	32	1.7	22	(12)	32
5×10^6	92	9.0	47	(54)	90
1×10^7	120	14	52	(82)	133
5×10^7	171	50	87	(134)	215

Discussion

Electronic States of Hot Ions. From the crystal field approximation, the ESR parameters of the d^7-low spin state in the C_{4v} (or D_{4h}) symmetry may be expressed as follows:[13]

$$g_{//} = 2.0023 \tag{1}$$

$$g_{\perp} = 2.0023 + 6\frac{\lambda}{\Delta} \tag{2}$$

$$A_{//} = P\left[-\kappa + \frac{4}{7} - \frac{6}{7}\frac{\lambda}{\Delta}\right] \tag{3}$$

Table 3. Some parameters derived from ESR measurements (using crystal field approximation)

	λ/Δ	$P(\mathrm{cm^{-1}})$	κ	$\lambda(\mathrm{cm^{-1}})$	$\Delta(\mathrm{cm^{-1}})$	χ	A_{iso}(G)	A_{aniso}(G)
Species I	0.0148	0.0168	0.215	340	23000	0.04	−36.5	100
Species II	0.0279	0.0173	0.0654	352	12600	0.06	−9.8	103

$$A_{\perp} = P\left[-\kappa + \frac{2}{7} - \frac{45}{7}\frac{\lambda}{\Delta}\right] \quad (4)$$

where $\Delta = E(z^2) - E$ (xz or yz), κ is an isotropic term, and λ is the spin-orbit coupling constant. The values calculated for λ/Δ, P, and κ from the experimental results listed in Table 1 are shown in Table 3, where $A_{//}$ and $A_{\perp}$ are assumed to have opposite signs. A comparison of the value of P (see Table 3) to that of the free ion P_0 (0.0254 $\mathrm{cm^{-1}}$) suggests that the unpaired electron is delocalized considerably in the orbital of the cyanide ligands (33%). This also gives rise to a smaller value of λ (see Table 3) than that for the free ion λ_0 (515 $\mathrm{cm^{-1}}$). With the consideration of the delocalization, the value of Δ for hot ions can be estimated from λ/Δ. Values of A_{iso} and A_{aniso} can also be calculated from $-P\kappa$ and $4/7P$, respectively. Symons and Wilkinson[14] gave an equation to derive the spin density χ in Co(4s): $A_{\mathrm{iso}}(\mathrm{G}) = 1320\chi - 90\leftarrow(1-\chi)$, where 1320 G is the theoretical value of A_{iso} from Co(4s) and 90 G is the $3d_{z^2}$ contribution to A_{iso} *via* spin polarization. χ was calculated by applying this relation. The values of χ, A_{iso}, and A_{aniso} are shown in Table 3. From the molecular orbital approximation, the ESR parameters of the d^7-low spin state in a C_{4v} (or D_{4h}) symmetry can be obtained as follows:[15]

$$g_{//} = 2.0023 \quad (5)$$

$$g_{\perp} = 2.0023 + 6\frac{\alpha^2\beta^2\lambda_0}{E(^2\mathrm{E}) - E(^2\mathrm{A}_1)} \quad (6)$$

$$A_{//} = P_0\left[-\kappa + \frac{4}{7}\alpha^2 - \frac{6}{7}\frac{\alpha^2\beta^2\lambda_0}{E(^2\mathrm{E}) - E(^2\mathrm{A}_1)}\right] \quad (7)$$

$$A_{\perp} = P_0\left[-\kappa + \frac{2}{7}\alpha^2 - \frac{45}{7}\frac{\alpha^2\beta^2\lambda_0}{E(^2\mathrm{E}) - E(^2\mathrm{A}_1)}\right] \quad (8)$$

The molecular orbitals are

$$^2\mathrm{A}_1(e^4b_2^2a_1^1) = \alpha d_{z^2} - d'\Phi_1(z^2) \quad (9)$$

$$^2\mathrm{E}(e^3b_2^2a_1^2) = \beta d_{xz}\ (\text{or } d_{yz}) - \beta'\Phi_1\ (\text{xz or yz}) \quad (10)$$

The values of P_0 and λ_0 for a free Co ion are calculated from atomic spectral data. They depend on their Co charge[16-18] (Table 4). From the optical spectrum[13]

Table 4. The values of P_0 and λ_0 for a Co ion they depend on the charge on the Co ion

Assumed Co charge	$P_0(\mathrm{cm^{-1}})$	$\lambda_0(\mathrm{cm^{-1}})$
Co^0	0.022[16]	390[18]
$Co^{+0.52}$	0.0224	424
Co^+	0.0228[17]	455[18]
Co^{2+}	0.0254[17]	515[18]

of $[Co^{II}(CN)_5]^{3-}$, $E(^2\mathrm{E}) - E(^2\mathrm{A}_1)$ has been determined to be 10350 $\mathrm{cm^{-1}}$. By substituting $E(^2\mathrm{E}) - E(^2\mathrm{A}_1)$, $\alpha^2\beta^2$, and the experimentally observed $g_{\perp}$ value into Eq. 6, λ_0, the charge of Co, and P_0 of hot ions are evaluated as 424 $\mathrm{cm^{-1}}$, +0.52, and 0.0224, respectively. With the values of $E(^2\mathrm{E}) - E(^2\mathrm{A}_1)$, P_0, λ_0, and $\alpha^2\beta^2$ thus fixed, the orbital coefficients α^2 and β^2 and the isotropic hyperfine interaction $-P_0\kappa$ can be calculated from Eqs. 7 and 8.

In the case of the hot ion $[Co^{II}(CN)_4(NC)_2]^{4-}$, substituting $\alpha^2\beta^2$, λ_0, and the experimentally obtained $g_{\perp}$ value into Eq. 6, $E(^2\mathrm{E}) - E(^2\mathrm{A}_1)$ is evaluated as 18900 $\mathrm{cm^{-1}}$. With the values of $E(^2\mathrm{E}) - E(^2\mathrm{A}_1)$, P_0, λ_0, and $\alpha^2\beta^2$ thus obtained, the orbital coefficients α^2 and β^2 and the isotropic hyperfine interaction $-P_0\kappa$ can be calculated from Eqs. 7 and 8. The calculated results are summarized in Table 5.

Table 5. Some parameters derived from ESR measurements (using molecular orbital approximation)

	$E(^2\mathrm{E}) - E(^2\mathrm{A}_1)$	α^2	β^2	$-P_0\kappa\ (\mathrm{cm^{-1}})$
Species I	18900	0.783	0.847	−0.00395
Species II	10350	0.826	0.826	−0.00171

According to the results shown in Tables 3 and 5, it is concluded that: i) the λ values for penta and hexa coordinated species are the same (about 350 $\mathrm{cm^{-1}}$); ii) the energy difference between the ground and the excited states is different for the two salts (about 10000 $\mathrm{cm^{-1}}$ for the pectacoordinated hot ion and about 20000 $\mathrm{cm^{-1}}$ for the hexacoordinated hot ion); and iii) the spin densities of hot ions are calculated as Co($3d_{z^2}$) 0.78 and Co(4s) 0.04 for species I, and Co($3d_{z^2}$) 0.83 and Co(4s) 0.06 for species II.

Mechanism of the Changes of Species I and II. *At 77K*: The mechanism of the reactions which take place in the γ-irradiated solid sample is assumed to take the scheme shown in Fig. 3. The secondary electrons which are formed by the γ-ray irradiation will hit Co^{III} in the complex of $[Co^{III}L_6]^{3-}$(1) in Fig. 3. With respect to the subsequent reactions, several different possible paths can be assumed. The first one is the case where the species(1) kicks out an electron, leaving itself as an positive hole. If the hole is stable, it will persist (3). If it is unstable, it may release one of the cyanide ligands,

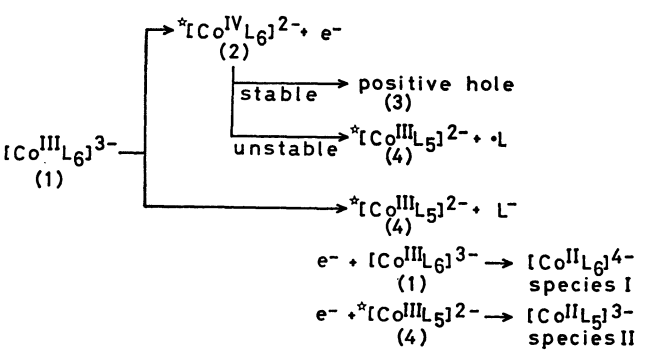

Fig. 3. The reaction mechanism at 77 K.
☆ stands for an excited species.

thus forming species (4). The latter can also be produced from species (1) directly. The active electron which is produced by the irradiation or by the process of the formation of (2) is trapped by (1) or (4), and produces hot ions.

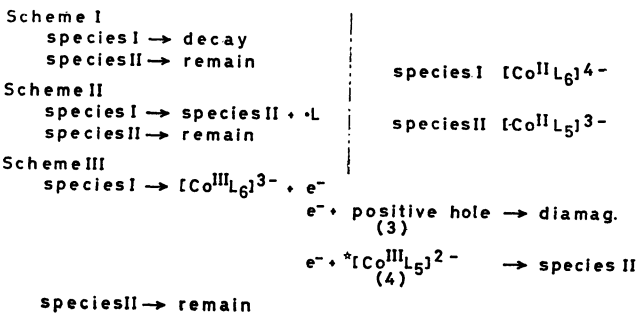

Fig. 4. The reaction mechanism on annealing.
☆ stands for an excited species.

On Annealing: From the experimental results, three processes of annealing can be imagined, as shown in Fig. 4. Among the processes shown in Fig. 4, we take scheme III as the most plausible. Scheme I cannot explain why the intensity of species II increases with temperature. Scheme II cannot explain the fact that some part of species I changes into the diamagnetic species. And of scheme II is the actual case, the formation of species II must be a first order reaction. In fact, this is against the experimental findings that both the formation of species II and that of the diamagnetic species are second order. But scheme III can explain the observed facts fairly well. According to this scheme, species I $[Co^{II}L_6]^{4-}$ releases an electron and returns to the original complex $[Co^{III}L_6]^{3-}$, and the electron thus released is trapped by another Co complex ion, such as $[Co^{IV}L_6]^{2-}$ (3) or $[Co^{III}L_5]^{2-}$ (4), forming either the diamagnetic ion or species II $[Co^{II}L_5]^{3-}$. Furthermore, the originally formed species II is kept unchanged according to this scheme.

Part II Single Crystal Experimental

Potassium hexacyanocobaltate(III) was prepared in the same way as in Part I from cobalt(II) chloride hexahydrate and potassium cyanide. Single crystals of $K_3[Co(CN)_6]$, approximately $3\times3\times1$ mm^3 in size, were obtained by slow evaporation of the aqueous solution. They were irradiated at 77 K with ^{60}Co γ-rays. 1×10^6 rads of γ-rays in total were applied to the sample at the rate of 5×10^4 rads/h. All conditions of the ESR measurements were the same as those in Part I. The crystals of $K_3[Co(CN)_6]$ exhibit polytypism.[19,20] Two unit cells occur in the structure of $K_3[Co(CN)_6]$: one, which is dominant, is orthorhombic (20 r) and the other monoclinic (1M,3M,7M). The ESR spectra observed in the present refer to the orthorhombic symmetry. The orthorhombic axes b and c of the crystal were easily identified with the aid of the crystallographic data,[21] and the axis of the right-handed orthorhombic system was unambiguously assigned. The ESR spectra were observed by rotating the sample at 15° intervals with the external magnetic field in the ab, ac, or bc plane.

Results

A typical example of the spectrum is shown in Fig. 5. It consists of one strong line due to the unidentified radicals, two wing lines (arrows) due to hydrogen atoms produced in the sample tube, and eight wing lines due to the Co(II) hot ions with a nuclear spin of 7/2. Two groups of octets are seen in the figure, which refer to two non-equivalent directions of the hyperfine tensor of the Co(II) hot ion. Each hyperfine line of cobalt is, furthermore, split into five lines, suggesting the coupling of cobalt with two equivalent nitrogen atoms. When the magnetic field was set parallel to the bc, ca, or ab planes, each spectrum became simple and revealed that it was formed of the two spectra shown in Figs. 5 and 6. Moreover, when the spectra taken at the arbitrary positions were analysed, taking this result into consideration, it was found that the spectra were produced by species I of the Co(II) hot ion located in four different sites in the unit cell. This means the produced hot ion is assigned as species I, which has been referred to in Part I, and is located at four sites in the unit cell of the mother lattice. The g-tensor was evaluated by measuring the central position between the first and the eighth peaks. The hyperfine coupling tensor was obtained as one-seventh of the separation between the first and eighth peaks. These results are shown in Fig. 7.

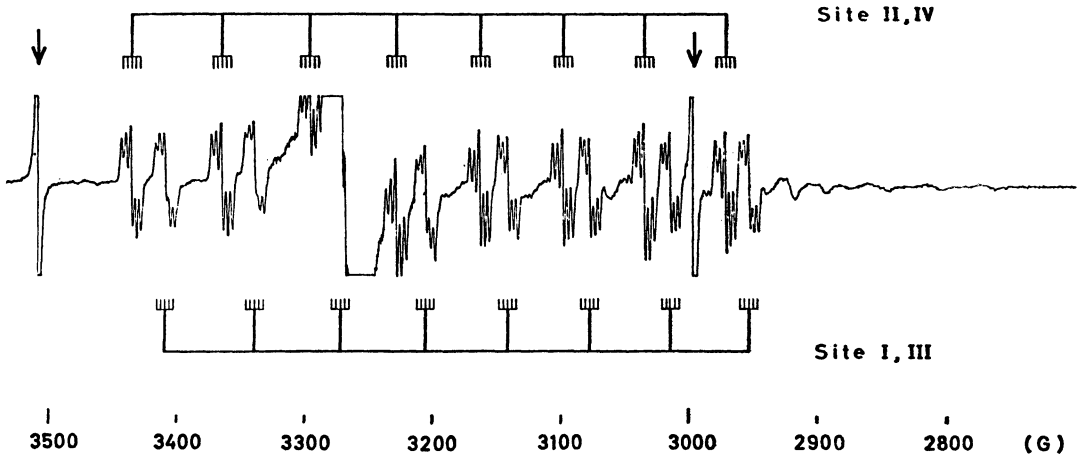

Fig. 5. An ESR spectrum of an irradiated single crystal of $K_3[Co(CN)_6]$ at 77 K.

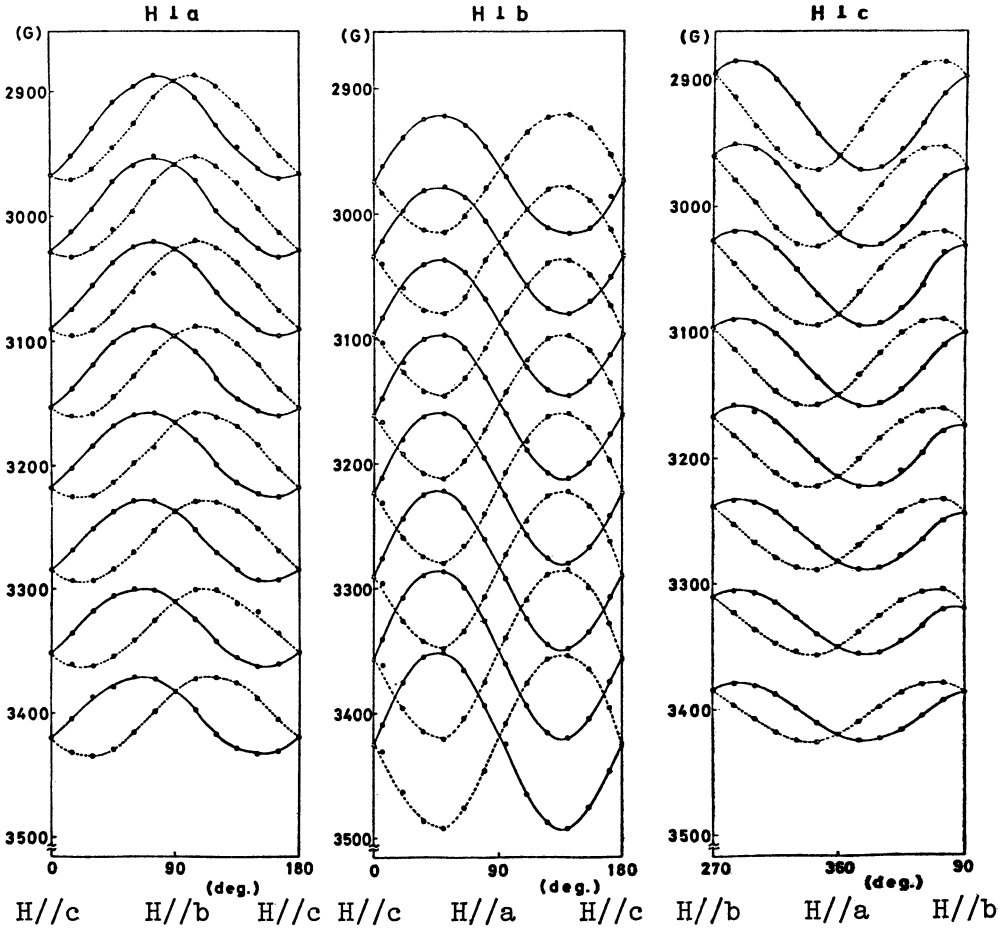

Fig. 6. The angular dependence of ESR spectra of irradiated single crystals of $K_3[Co(CN)_6]$ with orientation H being perpendicular to a, b, and c.

Discussion

Three different coordinate systems must be considered for the crystal of the sample: i) the crystallographic coordinate system (a, b, c), ii) the principal axis system of the g-tensor (α, β, γ), and iii) the principal axis system of the A-tensor (1, 2, 3). From the direction consines with respect to the magnetic field, the g values, and the hyperfine splitting K, the principal values and the principal of axes the g-tensor and the A-tensor are determined by the least-square method. The principal axes of the g-tensor do not necessarily coincide with those of the A-tensor. In the coordinates (α, β, γ), the g-tensor is diagonalized by

$$g^2 = (1_\alpha, 1_\beta, 1_\gamma) \begin{pmatrix} G_{\alpha\alpha} & 0 & 0 \\ 0 & G_{\beta\beta} & 0 \\ 0 & 0 & G_{\gamma\gamma} \end{pmatrix} \begin{pmatrix} 1_\alpha \\ 1_\beta \\ 1_\gamma \end{pmatrix}$$

where $G_{\alpha\alpha}=g_{\alpha\alpha}^2$, $G_{\beta\beta}=g_{\beta\beta}^2$ and $G_{\gamma\gamma}=g_{\gamma\gamma}^2$
In the coordinates (1, 2, 3), the A-tensor can be diagonalized, but the g-tensor cannot.

$$g^2K^2 = (1_1, 1_2, 1_3) \begin{pmatrix} g_{11} & g_{12} & g_{13} \\ g_{21} & g_{22} & g_{23} \\ g_{31} & g_{32} & g_{33} \end{pmatrix} \begin{pmatrix} B_{11} & 0 & 0 \\ 0 & B_{22} & 0 \\ 0 & 0 & B_{33} \end{pmatrix} \begin{pmatrix} g_{11} & g_{21} & g_{31} \\ g_{12} & g_{22} & g_{32} \\ g_{13} & g_{23} & g_{33} \end{pmatrix} \begin{pmatrix} 1_1 \\ 1_2 \\ 1_3 \end{pmatrix}$$

where $B_{11}=A_{11}^2$, $B_{22}=A_{22}^2$, and $B_{33}=A_{33}^2$.
In the crystallographic coordinates, the principal values

Table 6. The principal values and tne direction cosines of the principal axes of $[Co^{II}(CN)_4(NC)_2]^{4-}$, compared with the direction cosines of Co–C_i bonds in undamaged complexes, $K_3[Co(CN)_6]$

direction cosines of Co–C_i bonds in undamaged complexes, $K_3[Co(CN)_6]$, calculated from Curry and Runciman's data.[21]

	a	b	c
Co–C_2	0.678	0.237	0.696
Co–C_1	−0.421	0.906	0.044
Co–C_3	−0.642	−0.325	0.694

The principal values and the direction cosines of the principal axes of $[Co^{II}(CN)_4(NC)_2]^{4-}$.

Principal values (G)		a	b	c
A_1	68.4	0.66	0.22	0.72
A_2	70.3	−0.34	0.94	0.02
A_3	61.3	−0.67	−0.26	0.69

Principal values		a	b	c
g_3	2.009	0.70	0.25	0.67
g_1	2.089			
g_2	2.091		⊥ wrt above	

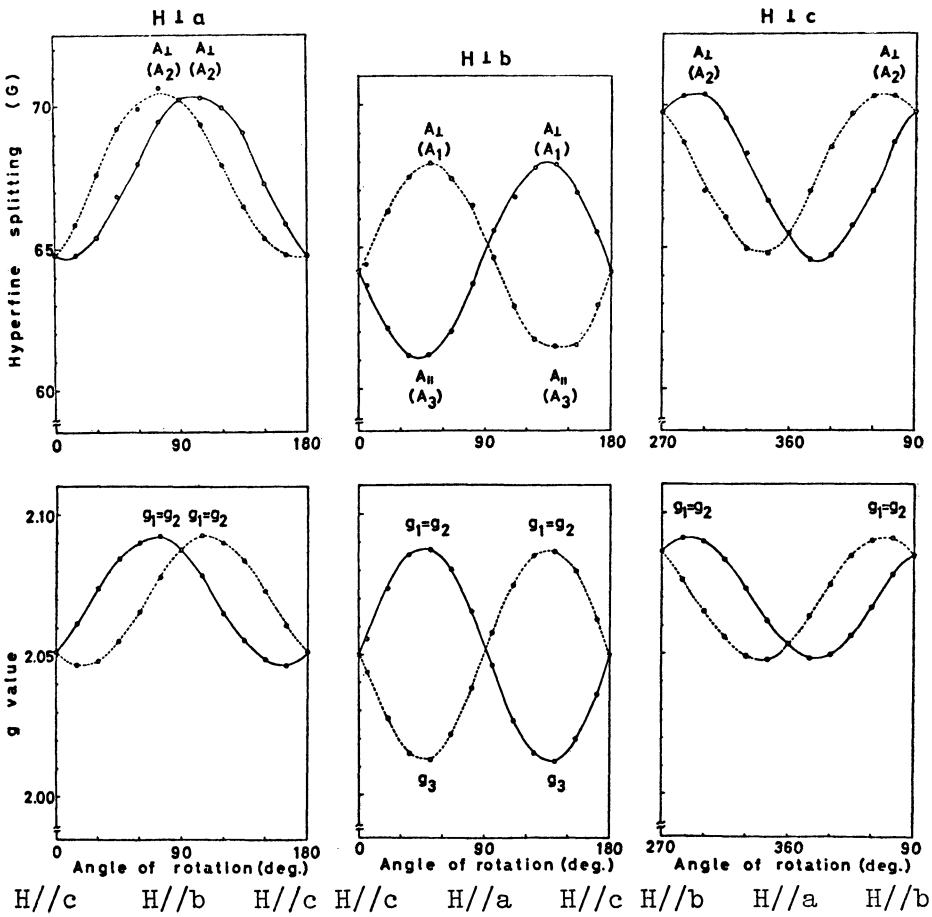

Fig. 7. The variation of hyperfine splitting and g values for irradiated single crystals of $K_3[Co(CN)_6]$ with the magnetic field H being perpendicular a, b, and c.

and the principal axes were determined (Table 6). The direction of the $A_{//}(A_3)$ axis coincides with Co–C_3 and the direction of the $g_{\shortparallel}(g_3)$ axis coincides with Co–C_2. Since $g_1 \simeq g_2 \simeq g_\perp$, the direction cosines of g_1 and g_2 cannot be determined exactly. Under the condition that the g-tensor and the A-tensor are axially symmetric, the parallel directions are orthogonal to each other. From the angular dependence of the superhyperfine splitting of nitrogen it is known that two cyanide ligands are inversed or twisted along the parallel direction of the g-tensor ($A^N_{//}=3.92$ G, $A^N_\perp=2.95$ G). Accordingly, the structure of the hot ion is axially symmetric along the $g_{//}$ axis. On the other hand, the distribution of the electron density is axially symmetric along the $A_{//}$ axis, *i. e.*, perpendicular to the $g_{//}$ axis. Similar noncollinear examples have been found in radicals,[22–24] but very rarely in metal complexes. Only five cases have been reported in the literature.[4,25–28] When the principal values and the principal axes of the g-tensor and the A-tensor are determined, the powder ESR spectrum can be assigned. As the parallel components of the g-tensor and the A-tensor are orthogonal, the $A_\perp$ can be seen at the $g_{//}$ part, and the $A_{//}$ and $A_\perp$ can be seen at the $g_\perp$ part (Fig. 8). Empirically it is known that $|A_{//}|<|A_\perp|$ for the hexacoordinated d^7-low spin complex, whereas $|A_{//}|>|A_\perp|$ for the pentacoordinated one.[1] Symons and his co-workers[8] reported that the g-tensor is

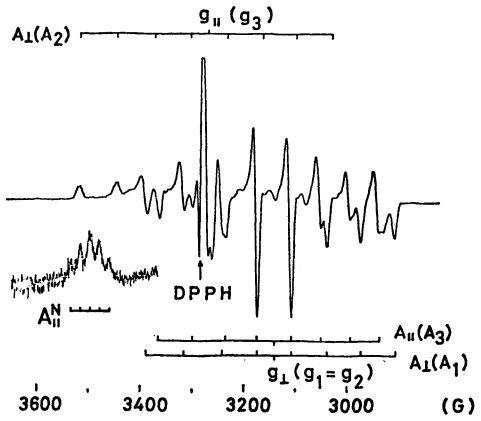

Fig. 8. An ESR powder spectrum of $[Co^{II}(CN)_4(NC)_2]^{4-}$. ESR parameters assigned by using the single crystal data. The superhyperfine structure at the $g_{//}$ part is caused by two equivalent nitrogen atoms of ligands.

axially symmetric ($g_x=g_y$) but the A-tensor is anisotropic ($A_x \neq A_y$). However, this statement is not right; both the g-tensor and the A-tensor are axially symmetric, and hence the principal axes do not coincide.

Other alkali metals were used instead of $3K^+$ to examine the effect of the mother lattice (Fig. 9). Species I can be measured only in the cases of $3K^+$ and $3Rb^+$.

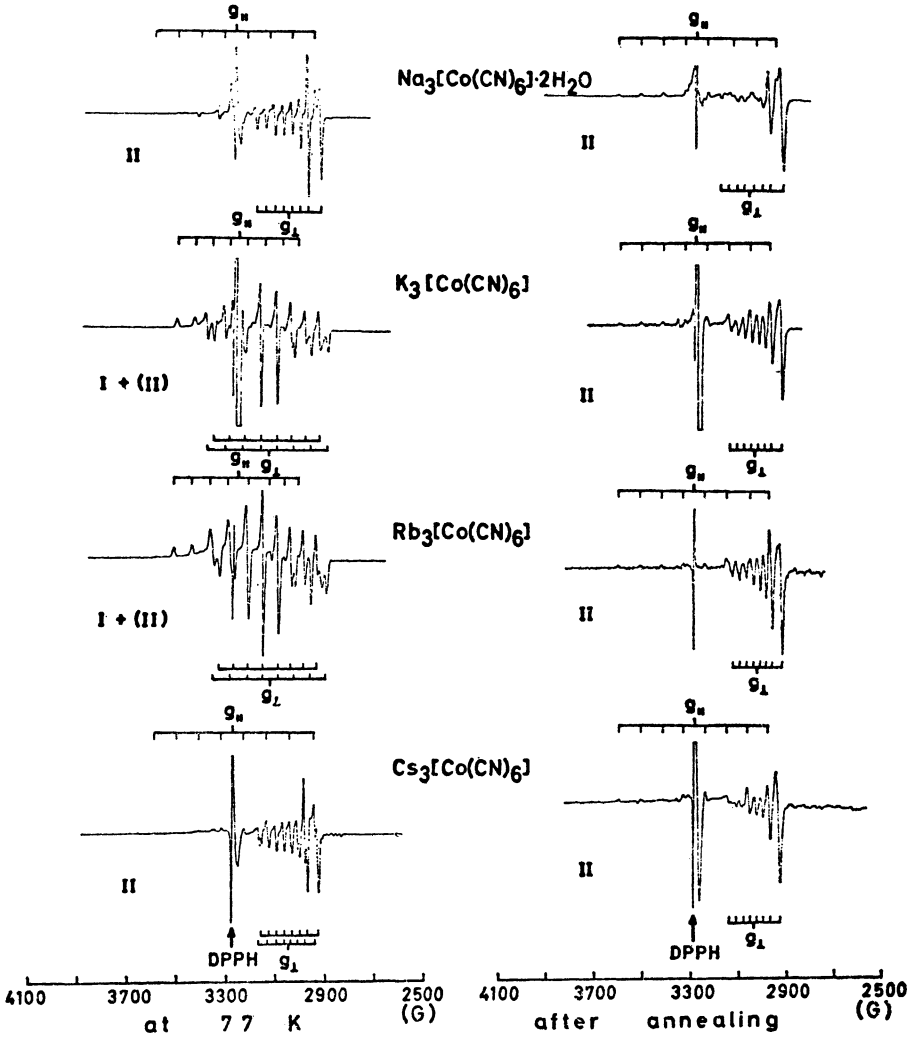

Fig. 9. ESR spectra of γ-irradiated powder of $M_3[Co(CN)_6]$ (M=Na, K, Rb, Cs).

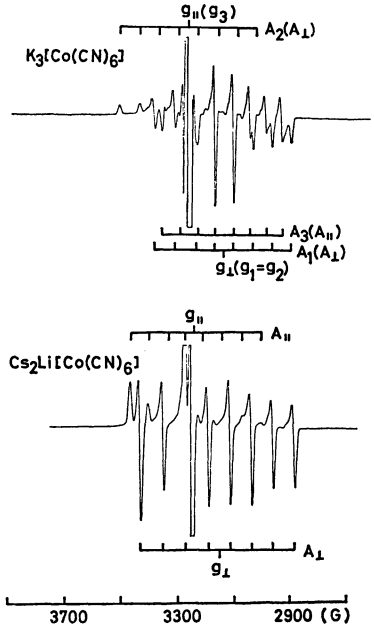

Fig. 10. ESR spectra of γ-irradiated powder of $K_3[Co(CN)_6]$ and $Cs_2Li[Co(CN)_6]$.

When the cation is changed from $3K^+$ to $2Cs^+Li^+$, the crystal system changes from orthorhombic to cubic. ESR parameters of hot ions produced in γ-irradiated $Cs_2Li[Co(CN)_6]$ at 77 K are shown in Table 7 for

TABLE 7. ESR PARAMETERS OF HOT IONS PRODUCED IN γ-IRRADIATED $K_3[Co(CN)_6]$ AND $Cs_2Li[Co(CN)_6]$.

	$g_{//}$	$A_{//}$(G)	$g_\perp$	$A_\perp$(G)
$Cs_2Li[Co(CN)_6]$	2.025	64	2.078	−78.1
$K_3[Co(CN)_6]$	2.011	61.7	2.091	−70.0

comparison with the case of $K_3[Co(CN)_6]$. In the case of $Cs_2Li[Co(CN)_6]$, no superhyperfine structures due to nitrogen atoms were observed. The $A_\perp$ can be seen at the $g_\perp$ part, and the $A_{//}$ can be seen at the $g_{//}$ part (Fig. 10). It can be concluded that the noncollinearity of the g-tensor and the A-tensor is not due to the local nature of the central metal, but to the entire nature of the mother lattice of the compound.

We wish to thank Mr. Shingo Katsura of the γ-ray irradiation center for his experimental assistance. We wish also to thank Dr. Yoji Arata and Dr. Jun-ichi Isoya for their helpful discussion.

References

1) S. Fujiwara, T. Watanabe, and H. Tadano, *J. Coord. Chem.*, **1**, 195 (1971).
2) J. Isoya and S. Fujiwara, *Bull. Chem. Soc. Jpn.*, **45**, 2181 (1972).
3) J. Isoya, H. Ishizuka, A. Yamasaki, and S. Fujiwara, *Chem. Lett.*, **1972**, 397.
4) N. S. Dalal, J. A. Hebden, and C. A. McDowell, *J. Magn. Resonance*, **16**, 289 (1974).
5) N. S. Dalal, J. A. Hebden, and C. A. McDowell, *J. Magn. Resonance*, **16**, 312 (1974).
6) J. Danon, R. P. A. Muniz, A. O. Caride, and I. Wolfson, *J. Mol. Struct.*, **1**, 127 (1968).
7) A. O. Caride, S. I. Zanette, and J. Danon, *J. Chem. Phys.*, **52**, 4911 (1970).
8) M. C. R. Symons and J. G. Wilkinson, *J. Chem. Soc., A*, **1972**, 1086.
9) J. R. Shock and M. T. Rogers, *J. Magn. Resonance*, **18**, 157 (1975).
10) W. C. Fernelius, *Inorg. Synth.*, Vol. II, McGraw-Hill New York (1946), p. 225.
11) J. P. Maher, *J. Chem. Soc., A*, **1968**, 2918.
12) M. E. Kimball, D. W. Pratt, and W. C. Kaska, *Inorg. Chem.*, **7**, 2006 (1968).
13) F. D. Tasay, H. B. Gray, and J. Danon, *J. Chem. Phys.*, **54**, 3760 (1971).
14) M. C. R. Symons and J. G. Wilkinson, *J. Chem. Soc., A*, **1971**, 2069.
15) R. J. Booth and W. C. Lin, *J. Chem. Phys.*, **61**, 1226 (1974).
16) A. Abragam and M. H. L. Pryce, *Proc. R. Soc. London*, **206**, 173 (1951).
17) B. R. McGarvey, *J. Phys. Chem.* **71**, 51 (1967).
18) T. M. Dunn, *Trans. Faraday Soc.*, **57**, 1441 (1961).
19) J. A. Kohn and W. D. Towns, *Acta Crystallogr.*, **14**, 617 (1961).
20) E. C. Reynfardt and J. C. A. Boeyens, *Acta Crystallogr.*, **B28**, 524 (1972).
21) N. A. Curry and W. A. Runciman, *Acta Crystallogr.*, **12**, 674 (1959).
22) R. W. Holmberg, *J. Chem. Phys.*, **51**, 3255 (1969).
23) E. L. Cochran, F. J. Adrian, and V. A. Bowers, *J. Chem. Phys.*, **44**, 4626 (1966).
24) R. M. Golding and W. C. Tennant, *Mol. Phys.*, **25**, 1163 (1973).
25) R. Byfleet, F. G. Herring, W. C. Lin, C. A. McDowell, and D. J. Ward, *Mol. Phys.*, **15**, 239 (1968).
26) J. G. Van Rens, C. P. Keijzers, and H. van Willigen, *J. Chem. Phys.*, **52**, 2858 (1970).
27) R. H. Borcherts and C. Kikuchi, *J. Chem. Phys.*, **40**, 2270 (1964).
28) J. R. Pilbrow and M. E. Winfield, *Mol. Phys.*, **25**, 1073 (1973).